

## Structure and Dynamics of a Metallic Glass: Molecular-Dynamics Simulations

R. N. Barnett, C. L. Cleveland, and Uzi Landman

*School of Physics, Georgia Institute of Technology, Atlanta, Georgia 30332*

(Received 21 June 1985)

The glass transition, structure, and dynamics of a  $\text{Ca}_{67}\text{Mg}_{33}$  metallic glass are studied via a new molecular-dynamics method incorporating the density dependence of the potentials. Results are in agreement with neutron-scattering data. The accessible configurational energy of the glass is found to possess several nearly degenerate potential minima.

PACS numbers: 61.20.Ja, 61.40.Df

Metallic glasses, i.e., the amorphous solid phases formed when segregation and crystallization are avoided by ultrarapid cooling of the liquid alloys, are the subject of much recent research effort because of their unique physical properties, which are of joint scientific and technological interest.<sup>1</sup> Metallic glasses are distinct from many other glass-forming materials because of the lack of bond-network entanglement commonly present in nonmetal-based glasses. Their stability and ease of formation have been correlated with electronic effects<sup>2</sup> and with metal-alloy chemistry and eutectic composition.<sup>3</sup>

Underlying the structural and dynamic properties of materials are the various contributions to the total potential energy, which for a metal alloy can be written as<sup>4</sup>

$$\Phi = E_{\Omega}(r_s) + \frac{1}{2} \sum'_{i,j} \phi_{ij}^{(2)}(r_s; |\mathbf{r}_i - \mathbf{r}_j|) + \dots, \quad (1a)$$

$$E_{\Omega}(r_s) = \sum_{\sigma} N_{\sigma} [Z_{\sigma} E_{el}(r_s) + \phi_0^{(1)}(r_s)], \quad (1b)$$

where  $\mathbf{r}_i$  is the position of the  $i$ th atom,  $Z_{\sigma}$  and  $N_{\sigma}$  are the valence and number of atoms of species  $\sigma$ ,  $r_s$  is the conduction-electron-density parameter,  $E_{el}$  is the energy per electron of a uniform electron gas,<sup>5</sup> and  $\phi^{(1)}$  and  $\phi^{(2)}$  are *density-dependent* single-particle and effective pair-interaction potentials. For simple (i.e.,  $s$ - $p$  bonded) metals, Eq. (1a) may be truncated after the second-order (pair-potential) terms, but for other metals, higher-order terms may be necessary.  $\phi^{(1)}$  and  $\phi^{(2)}$  may be derived via pseudopotential theory,<sup>6</sup> and their specific form depends upon the choice of ionic pseudopotential.<sup>7</sup>

Most previous computer studies of metallic glasses have employed "generic" pair potentials (such as Lennard-Jones, Morse, etc.).<sup>8</sup> While these studies have contributed to our understanding, they do not lend themselves to comparison with experimental results for a specific material and thus do not afford a *direct* critical assessment of the physical model and numerical procedure employed. Studies using more realistic potentials have been based on random-packing models (RPM) for the glass structure<sup>3,9</sup> and thus cannot address questions involving the kinetics and

dynamics of the glass transition itself or the dependence of metallic glass properties on thermal history, spatial fluctuations in concentration, or temporal fluctuations in local density and stress<sup>10</sup> and in the underlying glass structure.

A fundamental question in relating computer-simulated to laboratory-prepared glasses is the short time scale of computer simulations in comparison to the experimental ones.<sup>11,12</sup> It has been demonstrated<sup>12</sup> that, although the glass transition is broadened by the very rapid cooling rates used in computer simulations, it can be unambiguously observed and the dependence of quantities such as volume and internal energy on thermal history is small, and that trends may be extrapolated to experimental cooling rates. Thus, short of the performance of simulations employing laboratory cooling rates, an assessment of the correspondence between simulation and experimental results may be provided by simulations which employ a *realistic* description of the energetics for *specific* metallic glass systems for which extensive experimental data are available.

In order to perform a realistic dynamic simulation of the formation and properties of a metallic glass, we have developed a new molecular-dynamics (MD) formulation.<sup>4</sup> In our method the density dependence of both the volume energy,  $E_{\Omega}$ , and the pair potentials,  $\phi^{(2)}$ , is explicitly included in the Lagrangean from which the equations of motion are derived. The MD calculational cell volume (and optionally the shape) respond to differences between the internal and externally applied stress tensors,<sup>4,13</sup> and the potentials are *dynamically adjusted* in accord with the instantaneous density. Therefore, this method allows isoenthalpic simulations of processes, such as glass formation, which inherently involve changes in density, without one's having to specify the density at which the pair potentials are evaluated or applying an external "electronic" pressure to account partially for the volume energy.

Temperature control, i.e., cooling, heating, or equilibrating at a specified temperature, is accomplished by inclusion in the Lagrange equations of a "dissipation function"  $F(t, \{\dot{\mathbf{r}}_i\}) = A(t)T(\{\dot{\mathbf{r}}_i\})$ ,

where  $t$  is time,  $T$  is the instantaneous kinetic temperature (a function of particle velocities<sup>4</sup>), and  $A(t)$  is a "viscous damping" coefficient, given by  $A(t) = C[T(t) - T_0(t)]/T(t)$ , taken to be a function of time but not explicitly of particle velocities.  $T_0(t)$  is the "heat reservoir" temperature which may be a specified function of time yielding a well-defined continuous heating or cooling rate  $\dot{T}_0(t)$ .

A most sensitive probe of the nature of interatomic forces, and the structure (on various length scales) and dynamics of a glass-forming alloy, is provided by the static and dynamic structure factors obtained from neutron-scattering experiments.<sup>1b</sup> To assess critically the structural and dynamical information obtained by our new molecular-dynamics simulation method, we have chosen to study the metallic glass  $\text{Ca}_{67}\text{Mg}_{33}$ , a simple metal glass for which such neutron-scattering data are available,<sup>14</sup> and which has been investigated extensively with use of a random-packing model.<sup>9</sup> Our simulation, which is the first such realistic MD simulation of a metallic glass, affords a direct comparison with experiment and provides a faithful description of the material, and our results are in agreement with the experimental data and the principal theoretical results of Hafner.<sup>9</sup> In addition we found that the fully dynamically relaxed glass can be characterized by several nearly degenerate local potential minima. Transitions between these configurations involve large displacements by a small number of atoms.

The simulated system consisted of 500 particles, 333 Ca and 167 Mg atoms contained in a fixed-shape, variable-volume, regular rhombic dodecahedral MD cell.<sup>4</sup> The system of units which we use is [length] =  $a_0$  (Bohr radius), [mass] = amu (atomic mass unit), and [energy] = Ry, yielding a time unit (tu) =  $1.46 \times 10^{-15}$  sec.

The simulation was performed in four stages (all at zero external pressure): (1) an equilibrium run (with no temperature control) for the hot liquid alloy at  $T = 0.01$  Ry (1580 K, approximately twice the experimental eutectic temperature), for  $3 \times 10^4$  tu; (2) a "cooling" run of  $3 \times 10^4$  tu,  $\dot{T}_0 = 3 \times 10^{-7}$  Ry/tu ( $3.2 \times 10^{13}$  K/sec), during which the glass transition occurred; (3) an "equilibrating" run of  $14 \times 10^4$  tu in duration under temperature control at  $T_0 = 0.00191$  Ry (300 K) during which structural relaxation of the glass occurred [the mean square displacement of atoms during the run,  $R^2(t) = N^{-1} \sum [r_i(t) - r_i(0)]^2$ , increased in distinct steps while the internal energy decreased]; and (4) an equilibrium run for the glass at  $T = 0.00191$  Ry (without temperature control) of  $9 \times 10^4$  tu. The MD integration time-step size for stages (1) and (2) was  $\Delta t = 1$  tu, while in the glass,  $\Delta t = 2.5$  tu.

The principal effects of the increase in density in going from the liquid ( $r_s = 3.350a_0^{-3}$ ) to the glass

( $r_s = 3.136a_0^{-3}$ ) are a decrease in depth of the potential minima and a shift to shorter interatomic distance of the Friedel oscillations in the long-range part.<sup>4</sup> In addition the relative depths of the potentials are altered. The "electronic pressure,"  $r_s [\partial E_\Omega(r_s) / \partial r_s] / \Omega$ , increases from  $2.0 \times 10^{-4}$  Ry/ $a_0^3$  in the liquid to  $2.3 \times 10^{-4}$  Ry/ $a_0^3$  in the glass.

The evolution of the system during cooling (stage 2) is shown in Fig. 1. In Fig. 1(a) the mean square displacement,  $R^2(t)$ , and the kinetic temperature,  $T(t)$ , as functions of time are shown, while Fig. 1(b) shows the (per particle) total internal energy and the potential energies for the two species as functions of temperature [Fig. 1(b) was obtained by performing Gaussian-weighted local averages in time (Gaussian width of 1500 tu)]. From the break in the slopes of energy versus  $T$ , we determine the glass-transition temperature to be  $T_g = 0.0036$  Ry (570 K). A similar break in the slope of the volume  $\Omega$  vs  $T$  occurs at the same temperature. This value of  $T_g$  is about 0.7 times the experimental eutectic temperature, which is a typical value for measured glass-transition temperatures. Note that  $R^2(t)$  is constant for  $t > 2.3 \times 10^4$  tu, i.e., after the glass transition, and while the mean potential energies versus temperature for the two species have markedly different slopes above  $T_g$ , they have essen-

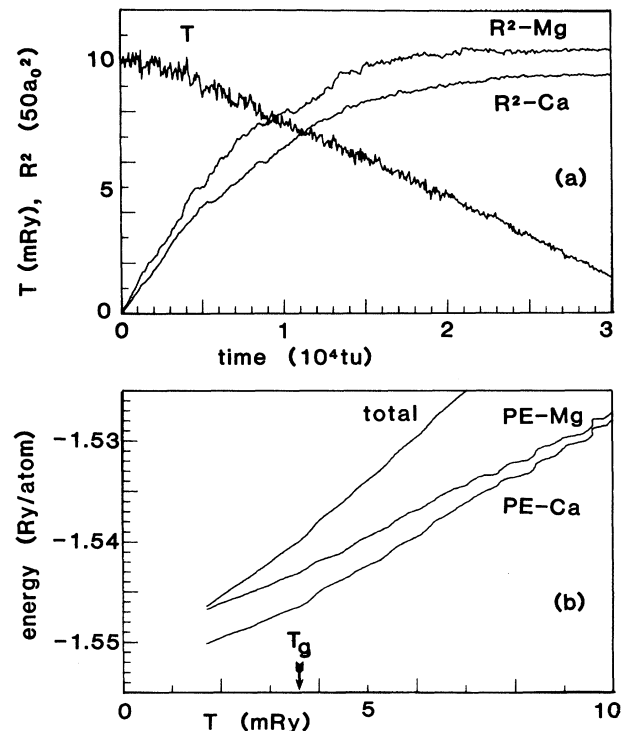


FIG. 1. System evolution during cooling: (a) temperature  $T$  and mean square displacement  $R^2$  vs time; (b) mean total energy and mean potential energies, PE, vs temperature.

tially the same slope below  $T_g$ , which is to be expected if the glass transition corresponds to a "freezing" of structural relaxation modes. Estimates of the specific heats of the supercooled alloy and glass can be obtained from the slopes of the total internal energy versus  $T$  in the two regions, yielding  $C_p/k_B=4$  and 3.3, respectively. These values are in approximate agreement with  $C_p/k_B=4.15$  for the initial equilibrium liquid and 3.16 for the final equilibrium glass obtained from fluctuations in the kinetic temperature.<sup>4,15</sup>

The structure and dynamics of the equilibrium glass are investigated via the radial pair-distribution functions,  $g(r)$ , and static structure factors,  $S(q)$ , as well as the density of states,  $\text{DOS}(\omega)$ , and dynamic structure factors,  $S(q, \omega)$ . For the glass, we observed correspondence between the locations of minima in the partial  $g(r)$ 's (not shown) and maxima in the corresponding pair potentials as discussed by Haftner.<sup>3</sup> Using the known neutron-scattering lengths  $b_{\text{Ca}}=4.88 \times 10^{-13}$  cm and  $b_{\text{Mg}}=5.2 \times 10^{-13}$  cm, we have calculated the neutron-weighted static and dynamic structure factors which may be compared directly with the experimental results<sup>14</sup> (we omit the incoherent-scattering contribution which is estimated<sup>14</sup> to be  $<1\%$ ). The positions of the first and second peaks of the static structure factor [Fig. 2(b)],  $Q_1=1.12a_0^{-1}$  and  $Q_2=1.92a_0^{-1}$ , are in good agreement with the reported experimental peak positions<sup>14</sup> ( $Q_1=1.13a_0^{-1}$  and  $Q_2=1.94a_0^{-1}$ ). The density of the simulated alloy,  $N/\Omega=0.00387a_0^{-3}$ , is also in good agreement with the experimental value<sup>9</sup> of  $0.00398a_0^{-3}$ . (This experimental value is presumably for a  $\text{Ca}_{70}\text{Mg}_{30}$  glass at 6 K. Indeed, a steepest-descent quench of our glass to 0 K results in a density of  $0.00397a_0^{-3}$ .) Figure 2(b) can also be compared to the relaxed RPM structure factor shown in Fig. 4 of Ref. 9. Note that  $g_{NN}(r)$  (defined by Bhatia and Thornton<sup>16</sup>) [Fig. 2(a)] exhibits a split second peak typical of a glass, and in addition there are indications

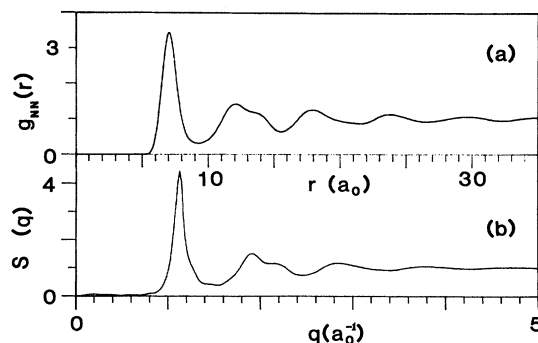


FIG. 2. Number density pair-correlation function  $g_{NN}(r)$  and neutron-weighted static structure factor  $S(q)$  for the glass.

of some amount of local order extending to at least the third-neighbor shell.

The density of states (DOS) and dynamic structure factor,  $S(q, \omega)$ , for the equilibrium glass are shown in Fig. 3. The structure factor is shown as a function of frequency,  $\omega$ , for wave vectors  $q_n = nq_1$ , where  $q_1 = 0.221a_0^{-1}$  is the magnitude of the (220) reciprocal lattice vector of the (fcc) lattice generated by the periodically replicated MD cell. The range of wave vectors  $q$  for which the structure factor has been reported by Suck *et al.*<sup>14</sup> corresponds roughly to  $q_3$  through  $q_{10}$  in Fig. 3; therefore, the calculated results can be compared with the experimental ones given in Fig. 3 of Ref. 14, showing general agreement of the line shapes as well as the frequency range (50 meV =  $0.111 \text{ tu}^{-1}$ ). Note in particular the increase in amplitude at low frequency for  $q \approx Q_1, 2Q_1$ , which has been attributed to transverse excitations, suggesting the existence of quasi zone boundaries in the glass.<sup>17</sup> From the positions of the peaks in  $S(q, \omega)$  for the

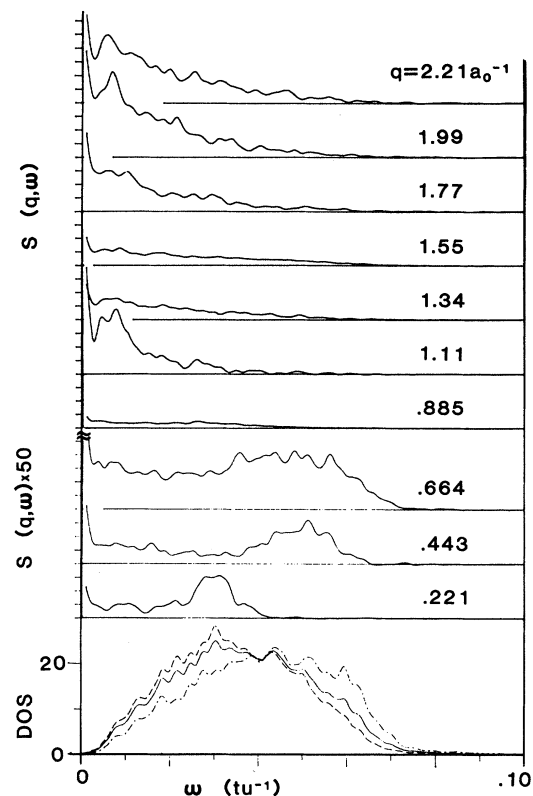


FIG. 3. Neutron-weighted dynamic structure factor  $S(q, \omega)$  in units of  $\text{tu}$  [each subdivision equals  $(2/\pi) \text{ tu} = 1.41 \times 10^{-3} \text{ meV}^{-1}$ ], vs frequency  $\omega$  (in  $\text{tu}^{-1}$ ), for wave vectors  $q$  as specified (note the scale change for  $q < 0.664a_0^{-1}$ ; the scale for each  $q$  starts at zero); and density of states  $\text{DOS}(\omega)$  (in  $\text{tu}$ ) (solid line, total; dashed line, Ca; dash-dotted line, Mg) vs  $\omega$  for the glass.

lower  $q$ 's in Fig. 3, we may read points on the dispersion curve for longitudinal phonons which are in agreement with the experimental results and with the theoretical dispersion curves obtained via the relaxed RPM.<sup>9</sup>

The density of states, obtained from the velocity autocorrelation function, is also in agreement with the experimental DOS (Fig. 11 of Ref. 9). The small oscillations at low frequencies are an artifact due to the periodic boundary conditions, complicating the discussion of the power-law behavior of the DOS at low frequencies. The peak in the DOS occurs at about  $0.032 \text{ tu}^{-1}$ , compared to  $0.033 \text{ tu}^{-1}$  found in the experiment ( $1 \text{ meV} = 0.002219 \text{ tu}^{-1}$ ). The full width at half maximum of our DOS is  $0.044 \text{ tu}^{-1}$ , compared to the experimental width of  $0.042 \text{ tu}^{-1}$ , while the width of Hafner's model DOS is  $0.051 \text{ tu}^{-1}$ . The difference between our DOS and the RPM result<sup>9</sup> occurs on the high-frequency side of the maximum where our DOS agrees better with the experimental data.

Having established via *direct* comparison with experimental data that our MD simulation in which the full energetics of the metallic system is self-consistently incorporated provides a faithful description of the structure and dynamics of the metallic glass system, we conclude with a brief discussion of observations relating to glass dynamics. Examination of the mean square displacement,  $R^2(t)$ , at the "equilibrated glass" stage (4) revealed time ranges when  $R^2(t)$  increased from about  $0.4a_0^2$  to about  $0.7a_0^2$ , then returned to the original lower value. These changes are accompanied by variations in system properties such as temperature, mean species potential energies, and average shear stress. By performing "steepest-descent quenches"<sup>18</sup> for these different time spans, we determined that the system possesses at least four distinct, nearly degenerate, local potential minima ranging from  $-1.551966$  to  $-1.551942$  Ry per atom. Comparison of the atomic positions associated with these potential minima reveals that they result from structural rearrangements in which, typically, one atom displaces by  $3a_0$  to  $4a_0$  (about half the average nearest-neighbor distance), the surrounding near-neighbor atoms move less, and the region of rearrangement extends over about three or four nearest-neighbor shells of the central atom, or about 15% to 20% of the total volume of the MD calculational cell. We emphasize that the transitions between these accessible local potential minima do not lead to an annealing or relaxation of the glass (over extended times), and that the underlying topology of the configurational energy is similar to that invoked in the "tunneling level" models of low-temperature glass behavior<sup>19</sup> (though the nature of our transitions is different). Further studies of the influence of these configurational transitions on glass prop-

erties and the dynamics near the glass transition are in progress.

This work was supported by the U.S. Department of Energy under Contract No. EG-S-05-5489.

<sup>1a</sup>Glassy Metals I, edited by H. I. Guntherodt and H. Beck (Springer, New York, 1981).

<sup>1b</sup>Glassy Metals II, edited by H. Beck and H. I. Guntherodt (Springer, New York, 1983).

<sup>1c</sup>S. R. Nagel, Adv. Chem. Phys. **51**, 227 (1982).

<sup>2</sup>S. R. Nagel and J. Tauc, Phys. Rev. Lett. **35**, 380 (1975); see also Ref. 1c.

<sup>3</sup>J. Hafner, Phys. Rev. B **21**, 406 (1981); see also Ref. 1a.

<sup>4</sup>R. N. Barnett, C. L. Cleveland, and U. Landman, Phys. Rev. Lett. **54**, 1679 (1985).

<sup>5</sup>P. Nozières and D. Pines, Phys. Rev. **111**, 442 (1958).

<sup>6</sup>See, e.g., W. A. Harrison, *Pseudopotentials in the Theory of Metals* (Benjamin, Reading, Mass., 1966); R. N. Barnett, R. G. Barrera, C. L. Cleveland, and U. Landman, Phys. Rev. B **28**, 1667 (1983); see also Ref. 3.

<sup>7</sup>For the simulation of the Ca-Mg alloy described in this paper, we used the simplified Heine-Abarenkov form described by Barnett, Cleveland, and Landman (Ref. 4) and by Barnett *et al.* (Ref. 6) with parameters chosen to give the correct zero-temperature lattice constant, cohesive energy, bulk modulus, and crystal structure of the pure species. The values of the parameters are  $r_c = 2.191a_0$ ,  $u_c = 0.415029$ ,  $Z_H = 1.11076$  for Ca, and  $r_c = 1.824a_0$ ,  $u_c = 0.548453$ ,  $Z_H = 0.940682$  for Mg.

<sup>8</sup>G. S. Grest, S. R. Nagel, and A. Rahman, Phys. Rev. B **29**, 5968 (1984); T. A. Weber, and F. H. Stillinger, Phys. Rev. B **31**, 1954 (1985); see also Refs. 1 and C. A. Angell, J. H. R. Clarke, and L. V. Woodcock, Adv. Chem. Phys. **48**, 397 (1981).

<sup>9</sup>J. Hafner, Phys. Rev. B **27**, 678 (1983); see also Refs. 1.

<sup>10</sup>T. Egami and D. Srolovitz, J. Phys. F **12**, 2141 (1982).

<sup>11</sup>See, e.g., Angell, Clarke, and Woodcock, Ref. 8.

<sup>12a</sup>J. R. Fox and H. C. Andersen, J. Phys. Chem. **88**, 4019 (1984).

<sup>12b</sup>M. H. Grabow and H. C. Andersen, in *Extended Abstracts, American Ceramic Society 87th Annual Meeting* (American Ceramic Society, Columbus, O. 1985), p. 160.

<sup>13a</sup>H. C. Andersen, J. Chem. Phys. **72**, 2384 (1980).

<sup>13b</sup>M. Parinello and A. Rahman, Phys. Rev. Lett. **45**, 1196 (1980).

<sup>14</sup>J.-B. Suck, H. Rudin, H. J. Guntherodt, and H. Beck, J. Phys. F **11**, 1375 (1981); see also Ref. 1b, p. 217.

<sup>15</sup>J. M. Haile and H. W. Graben, Mol. Phys. **40**, 1433 (1980).

<sup>16</sup>A. B. Bhatia and D. E. Thornton, Phys. Rev. B **2**, 3004 (1970).

<sup>17</sup>G. S. Grest, S. R. Nagel, and A. Rahman, Phys. Rev. B **29**, 5968 (1984).

<sup>18</sup>T. A. Weber and F. H. Stillinger, Phys. Rev. B **31**, 1954 (1985).

<sup>19</sup>See review by J. L. Black in Ref. 1b, p. 167.